Electronic Supplementary Material (ESI) for ChemComm

Page S1

Observation of a metal-doped B_2-Ta@B_{18}^- tubular molecular rotor and a Ta@B_{20}^- boron drums with the record coordination number of twenty

Wan-Lu Li,[a] Tian Jian,[b] Xin Chen,[a] Hai-Ru Li,[c] Teng-Teng Chen,[b] Xue-Mei Luo,[c] Si-Dian Li,*[c] Jun Li*[a] and Lai-Sheng Wang*[b]

[a] *Department of Chemistry and Key Laboratory of Organic Optoelectronics & Molecular Engineering of Ministry of Education, Tsinghua University, Beijing 100084 China*
junli@tsinghua.edu.cn
[b] *Department of Chemistry, Brown University, Providence, RI 02912 USA*
Lai-Sheng_Wang@brown.edu
[c] *Institute of Molecular Science, Shanxi University, Taiyuan 030006, China.*
lisidian@sxu.edu.cn

Table of Contents

Experimental and Computational Details

Photoelectron Spectroscopy Measurements: The experiment was carried out using a magnetic-bottle PES apparatus equipped with a laser vaporization supersonic cluster source, which has been described in detail elsewhere.[1] The TaB_{20}^{-} cluster was produced by laser vaporization of a composite target made of Bi/^{11}B/Ta. The Bi component was used as a binder and also provided a convenient source of Bi^{-} for calibration. Clusters formed in the nozzle were entrained by a He carrier gas seeded with 5% Ar and underwent a supersonic expansion to form a collimated cluster beam. Negatively charged clusters were extracted from the cluster beam and analyzed by a time-of-flight mass spectrometer. The TaB_{20}^{-} cluster of interest was mass-selected, decelerated, and photodetached by the 193 nm (6.424 eV) radiation from an ArF excimer laser or the fourth harmonic radiation (266 nm, 4.661 eV) from a Nd:YAG laser.Photoelectrons were collected at nearly 100% efficiency by a magnetic bottle and analyzed in a 3.5 meter long electron flight tube. The energy resolution of the apparatus was $\Delta Ek/Ek \approx 2.5\%$, that is, ~25 meV for 1 eV electrons.

Computational Details*:* Unbiased global minimum searches for both planar and three-dimensional TaB_{20}^{-} were carried out using the TGMin code.[14] More than 5000 trial structures were generated at the PBE/TZP level of theory using the ADF2013.01 software package.[2] Frozen core approximation was used for the inner shells of [$1s^2$] for B and [$1s^2$-$4d^{10}$] for Ta. The scalar relativistic (SR) and spin-orbit (SO) effects were taken into account by the zero-order-regular approximation (ZORA).[3] Low-lying energy isomers (ΔE< 35 kcal/mol) were further reoptimized at the PBE0/TZP level corrected by zero-point energies. Single-point energies were further refined for selected isomers at the PBE0 geometries using the CCSD(T) method implemented in Molpro2012.[4] Herein, the all-electron valence triple-ζ basis set cc-pVTZ (VTZ) was used for B. The relativistic 13-valence electron pseudopotential ECP60MDF and the corresponding cc-pVTZ-PP basis set was used for Ta. The binding energy between the central Ta and the B_{20} framework ($Ta + B_{20}^{-} \rightarrow Ta@B_{20}^{-}$) was also performed using the ROCCSD(T) method with the same basis sets.

The first vertical detachment energy (VDE) was calculated as the difference in energy between the anionic ground state and the neutral ground state at the anion geometry at the PBE, PBE0, and CCSD(T) levels with the inclusion of the SO effect. In all the CCSD(T) calculations, the T1 diagnosis factor was calculated to be around 0.018, indicating that single determinant methods should provide a sufficient description of the ground state wave functions. Higher VDEs were calculated using the TDDFT approach on the neutral species and then adding the first VDE. The TDDFT calculations were done with the statistically averaged orbital potential (SAOP), which could produce the correct asymptotic $1/r$ behavior.

Chemical bonding analyses were done on the drum-like isomer **2** using the AdNDP method with the Multiwfn code[5] generated from the PBE0/VTZ method, in order to obtain insight into the multicenter delocalized bonding. Molecular orbital (MO) visualization was performed using GaussView.[6] To understand the formation and transformation of isomer **1**, we searched for the transition state between two independent isomers utilizing the Gaussian09 program[7] at various DFT levels including PBE, PBE0, TPSSh,[8] M06-2X,[9] CAM-B3LYP,[10] as well as post-HF wave function methods of MP2[11] and CCSD(T) from Molpro 2012. Molecular dynamics (MD) simulations were performed at the PBE level using the CP2K software package.[12]

1 L. S. Wang, H. S. Cheng, J. Fan, *J. Chem.Phys.* 1995, **102**, 9480.

2 ADF, 2013.01, SCM, Theoretical Chemistry, Vrijie Universiteit, Amsterdam, The Netherlands, (http://www.scm.com).

3 E. van Lenthe, E. J. Baerends, J. G. Snijders, *J. Chem. Phys.* 1993, **99**, 4597-4610.

4 D. Y. Zubarev, A. I. Boldyrev, *Phys. Chem. Chem. Phys.* 2008, **10**, 5207-5217.

5 T. Lu, F. W. Chen, *J. Comput. Chem.* 2012, **33**, 580-592.

6 R. Dennington, T. Keith, J. Millam, GaussView, V. 4.1, Semichem, Inc., Shawnee Mission, KS, 2007.

7 M. J. Frisch, et al., gaussian 09, Revision B.01, Gaussian, Inc., Wallingford, CT, 2009.

8 V. N. Staroverov, G. E. Scuseria, J. Tao, J. P. Perdew, *J. Chem. Phys.* 2003, **119**, 12129-12137.

9 Y. Zhao, D. G. Truhlar, *Theo. Chem. Acc.* 2007, **120**, 215-241.

10 T. Yanai, D. P. Tew, N. C. Handy, *Chem. Phys. Lett.* 2004, **393**, 51-57.

11 C. Møller, M. S. Plesset, *Phys. Rev.* 1934, **46**, 618-622.

12 J. VandeVondele, M. Krack, F. Mohamed, M. Parrinello, T. Chassaing, J. Hutter, *Comput. Phys. Commun.* 2005, **167**, 103-128.

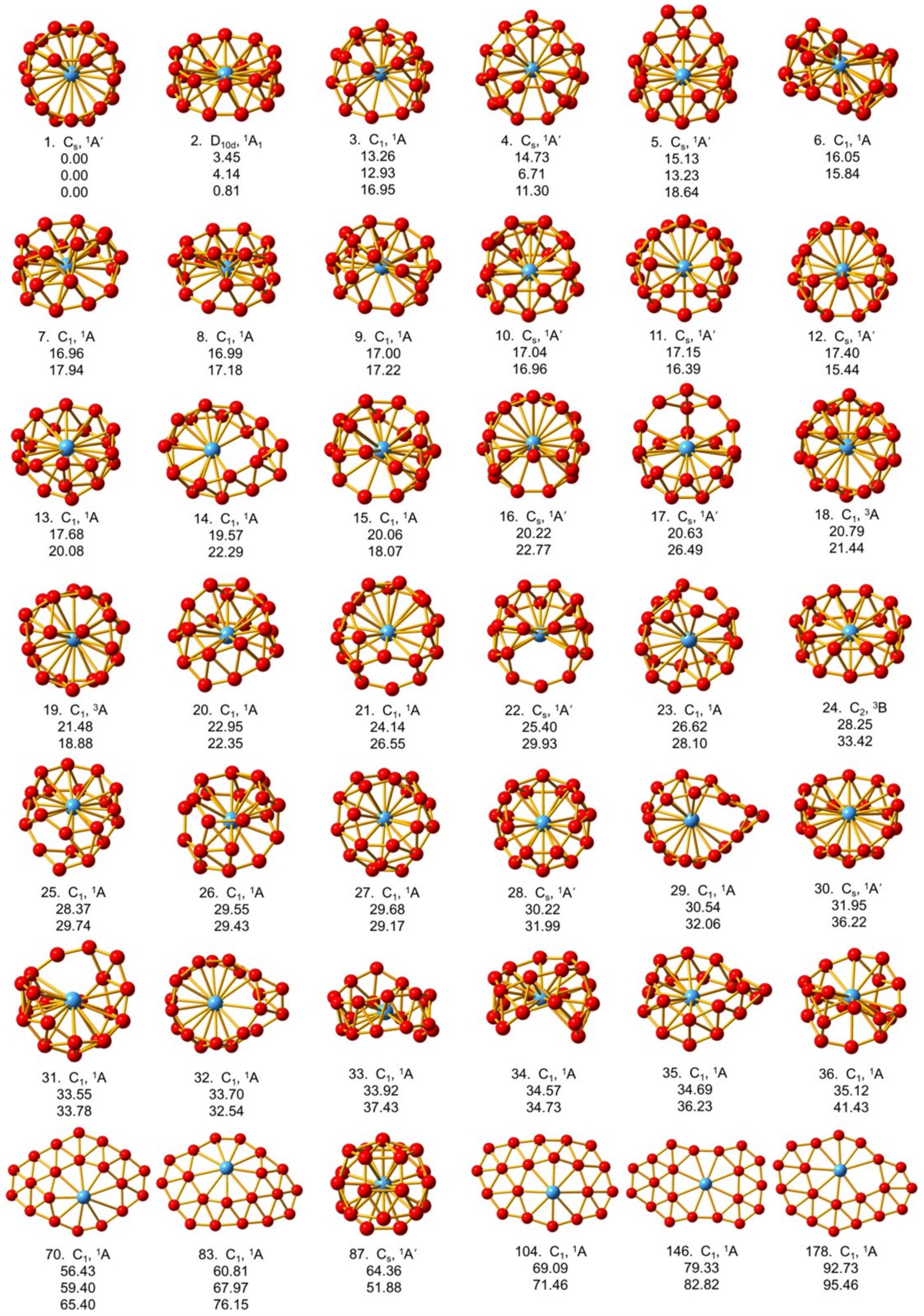

Figure S1. Optimized low-lying isomers of TaB_{20}^- within 35 kcal/mol of the global minimum at the PBE/TZP level, with their relative energies indicated in kcal/mol at the levels of scalar relativistic PBE0/TZP in the second rows and CCSD(T) in the third rows. Several quasi-planar structures with higher relative energies are also listed for comparison.

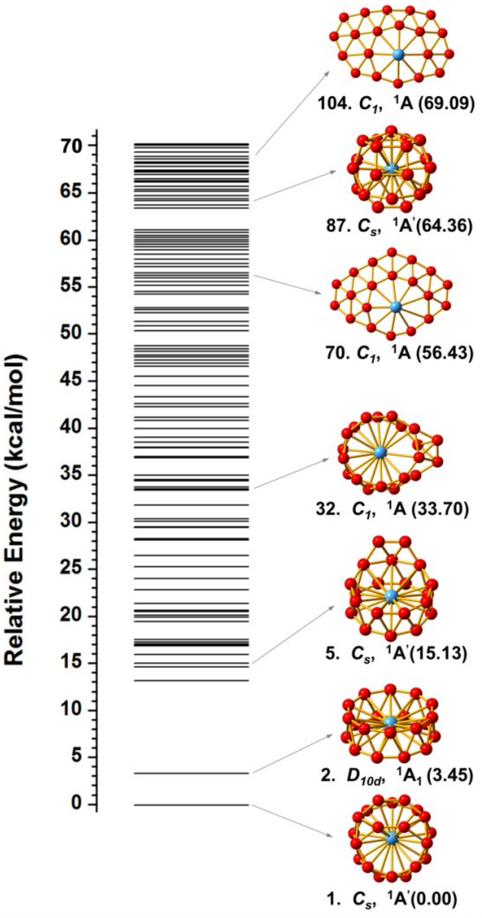

Figure S2. Configurational energy spectrum of TaB_{20}^- at PBE/TZP level.

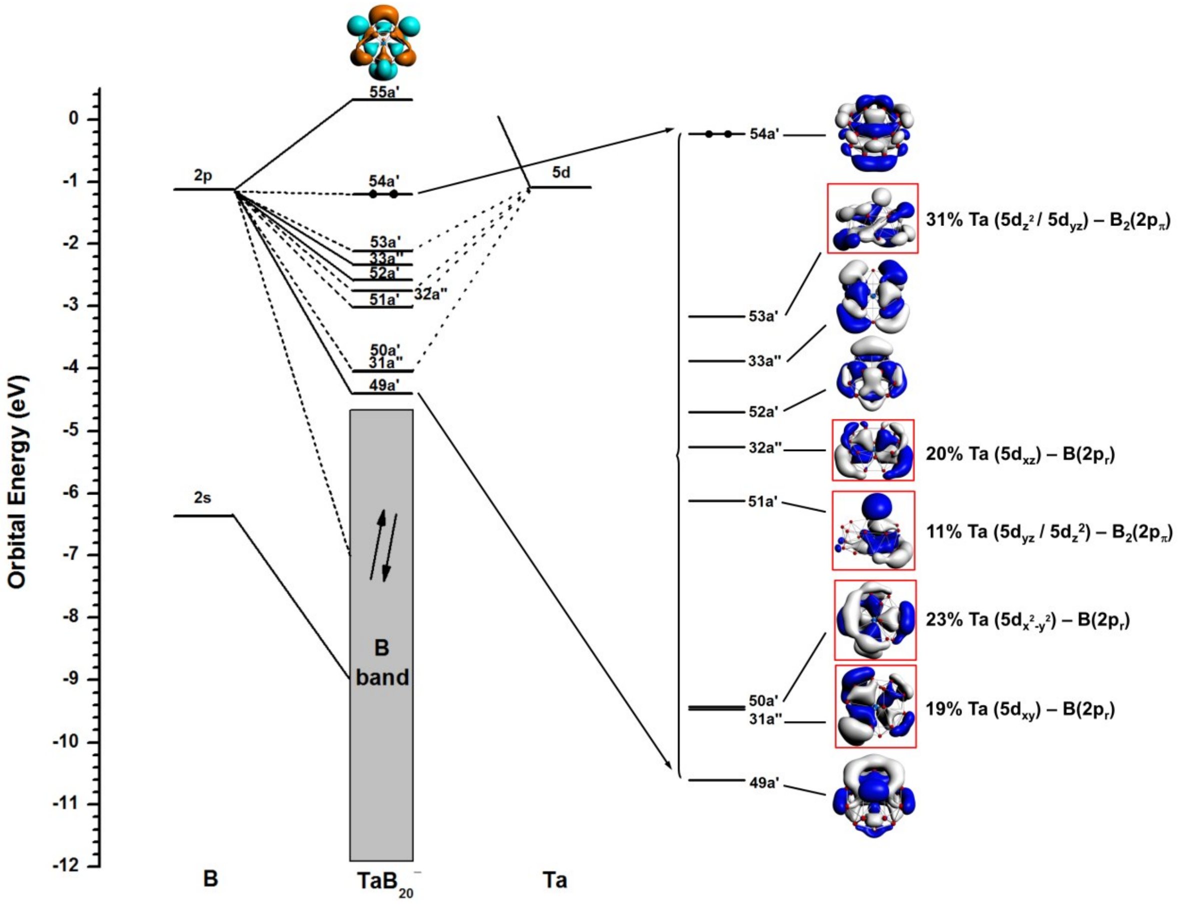

Figure S3. The MO level diagram for isomer **1** of TaB_{20}^- with the orbital pictures at the PBE/TZP level. The orbital with red frames correspond to the bonding orbitals between the central Ta and the B atoms. The subscript r represents the locally radial direction of the B_{18} drum.

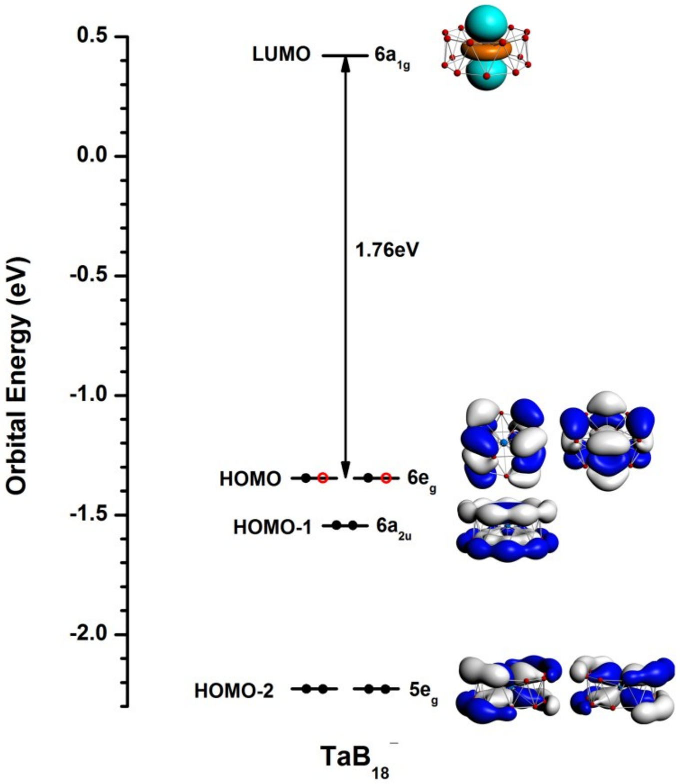

Figure S4. Molecular orbitals of TaB_{18}^- ($^3A_2$) at the PBE/TZP level. The two hollow circles in the HOMO indicate that two additional electrons are required to form a stable TaB_{18}^{3-} ($^1A_1$) cluster.

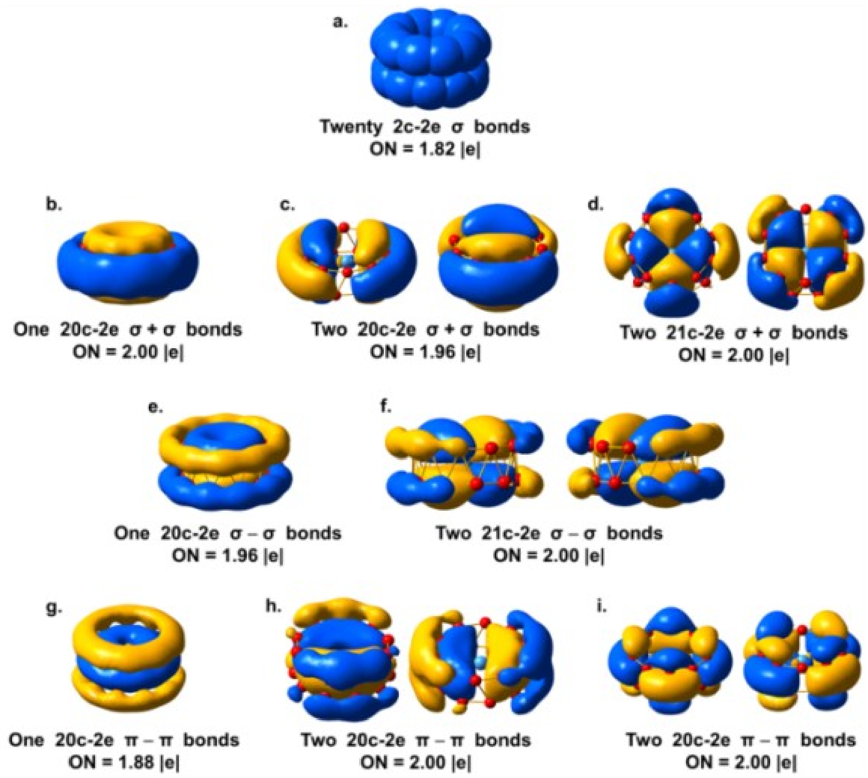

a. Twenty 2c-2e σ bonds ON = 1.82 |e|

b. One 20c-2e $\sigma+\sigma$ bonds ON = 2.00 |e|

c. Two 20c-2e $\sigma+\sigma$ bonds ON = 1.96 |e|

d. Two 21c-2e $\sigma+\sigma$ bonds ON = 2.00 |e|

e. One 20c-2e $\sigma-\sigma$ bonds ON = 1.96 |e|

f. Two 21c-2e $\sigma-\sigma$ bonds ON = 2.00 |e|

g. One 20c-2e $\pi-\pi$ bonds ON = 1.88 |e|

h. Two 20c-2e $\pi-\pi$ bonds ON = 2.00 |e|

i. Two 20c-2e $\pi-\pi$ bonds ON = 2.00 |e|

Fig.S5 AdNDP bonding pattern of D_{10d} Ta@B$_{20}^{-}$ (**2**). ON stands for occupation numbers.

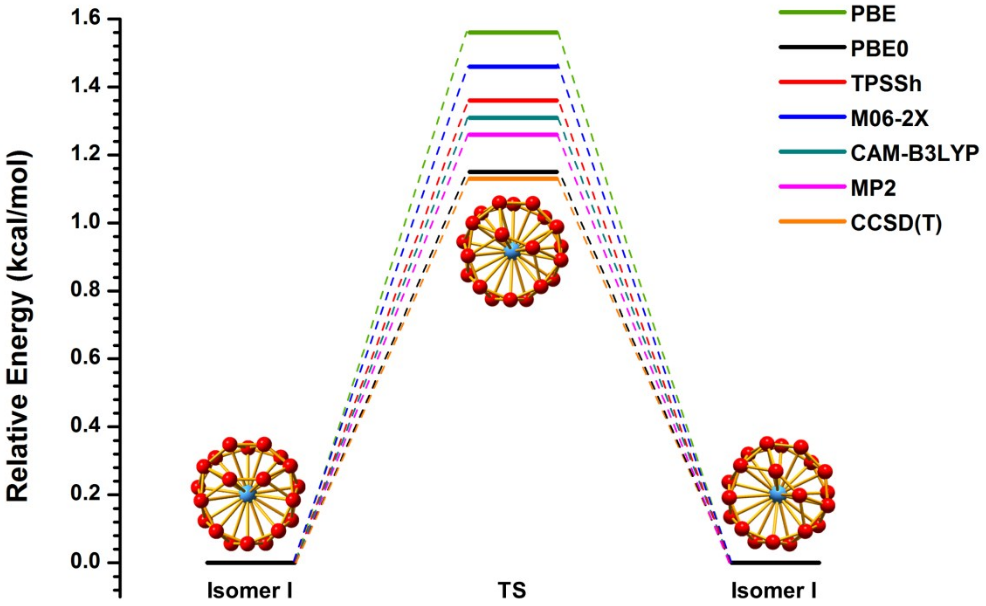

Figure S6. The rotational transition state (TS) barrier (kcal/mol) at different levels of theory for the global minimum of isomer **1** of TaB_{20}^{-}.

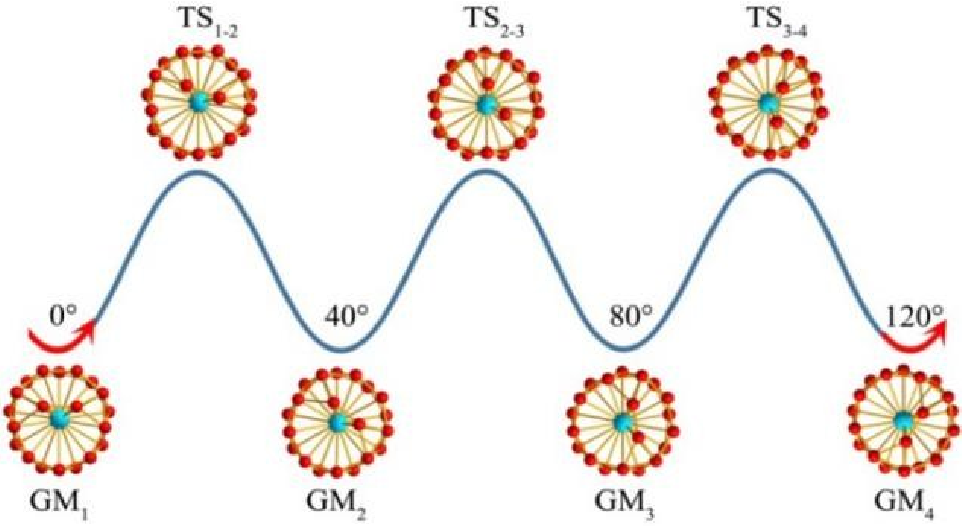

Fig.S7 Clockwise rotation of the B_2 unit in B_2-Ta@B_{18}^- (**1**) in one-third of a full circle. GM_i (i = 1−4) and $TS_{i\text{-}j}$ (i,j = 1−4) represent the global minima and the transition states, respectively, along the B_2 rotational path. The B_2 unit rotates 40° in one step with an energy barrier of 1.13 kcal/mol at CCSD(T).

Table S1. Theoretical VDEs (eV) from TDDFT/SAOP calculations for the isomer **1** and isomer **2** compared with the experimental results. VDE1 values are obtained from the CCSD(T) calculations.

Observed Features	VDE (Exp)	Final state and electronic configuration	VDE (Calc)
X	3.30(5)	Isomer **1** : $(^2\mathrm{A}')$ ... $49a'^2 50a'^2 31a''^2 51a'^2 32a''^2 52a'^2 33a''^2 53a'^2 \mathbf{54a'^1}$	3.14
X′	3.63(5)	Isomer **2** : $(^2\mathrm{A}_1)$ ...$13e_2^4 17e_1^4 18e_1^4 14e_2^4 \mathbf{21a_1^1}$	3.66
A	4.29(6)	Isomer **2** : $(^2\mathrm{E}_2)$ ...$13e_2^4 17e_1^4 18e_1^4 \mathbf{14e_2^3} 21a_1^2$	4.08
		Isomer **1** : $(^2\mathrm{A}')$ ... $49a'^2 50a'^2 31a''^2 51a'^2 32a''^2 52a'^2 33a''^2 \mathbf{53a'^1} 54a'^2$	4.23
		Isomer **1** : $(^2\mathrm{A}'')$ ... $49a'^2 50a'^2 31a''^2 51a'^2 32a''^2 52a'^2 \mathbf{33a''^1} 53a'^2 54a'^2$	4.32
		Isomer **2** : $(^2\mathrm{E}_1)$ ... $13e_2^4 17e_1^4 \mathbf{18e_1^3} 14e_2^4 21a_1^2$	4.49
B	4.86(6)	Isomer **1** : $(^2\mathrm{A}')$ ... $49a'^2 50a'^2 31a''^2 51a'^2 32a''^2 \mathbf{52a'^1} 33a''^2 53a'^2 54a'^2$	4.57
		Isomer **1** : $(^2\mathrm{A}'')$ ... $49a'^2 50a'^2 31a''^2 51a'^2 \mathbf{32a''^1} 52a'^2 33a''^2 53a'^2 54a'^2$	4.76
C	5.22(5)	Isomer **1** : $(^2\mathrm{A}')$ ... $49a'^2 50a'^2 31a''^2 \mathbf{51a'^1} 32a''^2 52a'^2 33a''^2 53a'^2 54a'^2$	5.21
D	6.0(1)	Isomer **1** : $(^2\mathrm{A}'')$ ... $49a'^2 50a'^2 \mathbf{31a''^1} 51a'^2 32a''^2 52a'^2 33a''^2 53a'^2 54a'^2$	6.02
		Isomer **2** : $(^2\mathrm{E}_1)$ ... $13e_2^4 \mathbf{17e_1^3} 18e_1^4 14e_2^4 21a_1^2$	6.08
		Isomer **2** : $(^2\mathrm{E}_2)$ ...$\mathbf{13e_2^3} 17e_1^4 18e_1^4 14e_2^4 21a_1^2$	6.26
		Isomer **1** : $(^2\mathrm{A}')$ ... $49a'^2 \mathbf{50a'^1} 31a''^2 51a'^2 32a''^2 52a'^2 33a''^2 53a'^2 54a'^2$	6.28
		Isomer **1** : $(^2\mathrm{A}')$ ... $\mathbf{49a'^1} 50a'^2 31a''^2 51a'^2 32a''^2 52a'^2 33a''^2 53a'^2 54a'^2$	6.41

Table S2: Calculated first VDEs and ADEs of isomers **1** and **2** for TaB_{20}^{-} at PBE, PBE0, and CCSD(T) levels, compared with the corresponding experimental values.

		Isomer **1**	Isomer **2**
VDE	PBE	3.02 (3.02)	3.49 (3.50)[a]
	PBE0	3.02 (3.03)	3.59 (3.60)
	CCSD(T)	3.14	3.66
	Exp.	3.30(5)	3.63(5)
ADE	PBE	2.86 (2.87)	3.42 (3.43)
	PBE0	2.87 (2.88)	3.49 (3.50)
	CCSD(T)	3.05	3.65
	Exp.	2.95(5)	-

[a] The numbers in parentheses are corrected with SO coupling.

Table S3. Different theoretical Ta-B bond orders calculated for the two global minimal isomers **1** and **2**.

		R (Ta−B)	Mayer[1]		Wiberg[2]		G-J[3]		N-M(1)[4,5]		N-M(3)	
			Each	Total	Each	Total	Each	Total	Each	Total	Each	Total
Isomer **1**	B_2 (top)	2.202	0.49	6.02	0.53	5.74	0.56	6.88	0.59	7.12	0.58	7.10
	B_{18}[a] (bottom)	2.496	0.28		0.26		0.32		0.33		0.33	
Isomer **2**		2.672	0.26	5.20	0.25	5.00	0.22	4.40	0.27	5.40	0.24	4.80

[a] The bond order of each Ta-B bond is the average value.

1 C. I. Mayer, *Chem. Phys. Lett.* 1983, **97**, 270-274.

2 K. B. Wiberg, *Tetrahedron.* 1968, **24**, 1083-1096.

3 M. S. Gopinathan, K. Jug, I. Valency, *Theor. Chim. Acta.* 1983, **63,** 497-509.

4 A. Michalak, R. L. DeKock, T. Ziegler, *J. Phys. Chem. A* 2008, **112**, 7256-7263.

5 R. F. Nalewajski, J. Mrozek, A. Michalak, *Int. J. Quantum Chem.* 1997, **61**, 589-601.

Table S4. List of the Cartesian coordinates of the two competing global minimum isomers **1** and **2** for TaB_{20}^- at the PBE0/TZP level.

Isomer 1 (C_s, $^1A'$)

Ta	0.897095	1.807675	1.462160
B	0.849419	2.401828	0.000000
B	0.737552	−1.234441	2.028945
B	0.947389	0.368782	2.160634
B	0.613349	−2.262698	−0.806952
B	0.613349	−2.262698	0.806952
B	0.897095	1.807675	−1.462160
B	0.947389	0.368782	−2.160634
B	0.737552	−1.234441	−2.028945
B	−0.990557	−1.705430	1.536499
B	−1.120494	−2.163910	0.000000
B	−0.751015	1.250550	2.026105
B	−0.836061	−0.315246	2.341239
B	−0.754603	2.327526	−0.810778
B	−0.754603	2.327526	0.810778

B	-0.990557	-1.705430	-1.536499
B	-0.836061	-0.315246	-2.341239
B	-0.751015	1.250550	-2.026105
B	1.755047	-0.590537	0.794245
B	1.755047	-0.590537	-0.794245
B	-0.202062	0.032023	0.000000

Isomer 2 (D_{10d}, $^1A_1$)

Ta	0.000000	0.000000	0.005587
B	-2.411812	0.783679	0.848758
B	-1.490613	2.051599	0.848758
B	0.000032	2.535939	0.848758
B	1.490562	2.051637	0.848758
B	2.411831	0.783618	0.848758
B	2.411831	-0.783618	0.848758
B	1.490562	-2.051637	0.848758
B	0.000032	-2.535939	0.848758
B	-1.490613	-2.051599	0.848758
B	-2.411812	-0.783679	0.848758
B	-2.535888	0.000000	-0.838072
B	-2.051757	1.490689	-0.837610
B	-0.783632	2.411772	-0.838072
B	0.783702	2.411985	-0.837610
B	2.051576	1.490557	-0.838072
B	2.536111	0.000000	-0.837610
B	2.051576	-1.490557	-0.838072
B	0.783702	-2.411985	-0.837610
B	-0.783632	-2.411772	-0.838072
B	-2.051757	-1.490689	-0.837610

Video S1